Couplings between the temporal and orbital angular momentum degrees of freedom in ultrafast optical vortices

Miguel A. Porras
Grupo de Sistemas Complejos, ETSIME, Universidad Politécnica de Madrid, Rios Rosas 21, 28003 Madrid, Spain

Claudio Conti
Institute for Complex Systems, CNR, Via dei Taurini 19, 00185 Rome, Italy
and Department of Physics, University Sapienza, Piazzale Aldo Moro 5, 00185 Rome, Italy

(Received 27 November 2019; revised manuscript received 24 March 2020; accepted 15 May 2020; published 1 June 2020)

In any form of wave propagation, strong spatiotemporal coupling appears when nonelementary three-dimensional wave packets are composed by superimposing pure plane waves or spontaneously generated by light-matter interaction and nonlinear processes. Ultrashort pulses with orbital angular momentum (OAM), or ultrashort vortices, furnish a critical paradigm in which the analysis of the spatiotemporal coupling in the form of temporal-OAM coupling can be carried out accurately by analytical tools. By generalizing and unifying previously reported results, we show that universal and spatially heterogeneous space-time correlations occur in propagation-invariant temporal pulses carrying OAM. In regions with high intensity, the pulse duration has a lower bound fixed by the topological charge of the vortex and such that the duration must increase with the topological charge. In regions with low intensity in the vicinity of the vortex, a large blueshift of the carrier oscillations and an increase of the number of them are predicted for strongly twisted beams. We think that these very general findings highlight the existence of a structural coupling between space and time. These results have also applications in free-space communications, spectroscopy, and high-harmonic generation.

DOI: 10.1103/PhysRevA.101.063803

I. INTRODUCTION

Since their first introduction in acoustics [1], propagation-invariant three-dimensional wave packets have attracted a great deal of attention because of fundamental issues, such as superluminality [2,3] and wave-function localization [4–6], and potential applications, for example, in telecommunications [7,8]. Solutions of wave equations evolving without distortion were also considered in Bose-Einstein condensation [9], linear and nonlinear optics [10,11], and more recently in polaritonics [12,13] and hydrodynamics [14]. X waves with orbital angular momentum (OAM) have been described recently as solutions of Maxwell equations [15,16], and quantum optical X waves [17] with OAM have been studied for their applications in free-space multilevel transmission systems (see [18] and references therein).

In spite of the relevance of X waves with OAM as the first reported ultrashort vortices with diffraction-free behavior, actual linear and nonlinear experiments with vortices in ultrafast (femtosecond or attosecond) regimes employ pulsed Laguerre-Gauss (LG) beams [19–23]. There has been increasing interest in synthesizing shorter and shorter vortices of the LG type [24–29], which in the high-intensity regime are used to generate high harmonics and attosecond vortices with high OAM [19–23]. From a theoretical point of view, it has been demonstrated recently [30–32] that pulsed LG beams with the so-called isodiffracting conditions [33] maintain a propagation-invariant pulse temporal shape as X waves, even if they are subject to diffraction.

Notwithstanding these many investigations, fundamental questions regarding ultrafast X and LG vortices remain unsolved. In recent years, a coupling between the temporal and OAM degrees of freedom in ultrashort (few-cycle and subcycle) pulses has been described theoretically in ultrafast X vortices [15,16] and LG vortices [30–32]. A consequence detailed in these works is that an arbitrarily short pulse cannot carry an arbitrarily high OAM, but there is a lower bound to its duration for given OAM. However, the effects of temporal-OAM coupling in ultrashort X and LG vortices appear to be quite different, even contradictory. The results in [15] show that in ultrafast X vortices the carrier frequency and the number of oscillations increase with angular momentum and that the increase of the carrier frequency is faster than the increase of the number of oscillations, so the pulse duration decreases with OAM. On the contrary, Refs. [30,31] report an absent or negligible blueshift for ultrafast LG vortices and an increase of the pulse duration with OAM.

Here we report a general and unified treatment for both types of ultrashort vortices with propagation-invariant pulse shape. First we show that the two analyses are not in contradiction because they refer to different spatial regions of the ultrashort vortex. Second we unveil a very rich phenomenology common to all ultrafast vortices with propagation-invariant pulse shape. We distinguish the effects of the temporal-OAM coupling depending on the model from those which are intrinsic or "universal." Our results have implications in perturbative nonlinear optics and high-field, nonperturbative,

light-matter interactions (as in high-harmonic and attosecond pulse generation experiments) and in quantum optics in the low photon regime. Indeed, in ultrafast propagation of twisted pulses, regions of high intensity (high energetic ring) and low intensity (central vortex core with phase singularity) are present and the nature of temporal-OAM coupling varies a great deal in these different portions of these three-dimensional wave packets. We describe below different experimentally testable features to demonstrate the heterogeneous spatiotemporal coupling in ultrashort vortices.

II. ULTRAFAST LAGUERRE-GAUSS AND *X* VORTICES

We express the optical field $E(r,\phi,t,z)$, or E for short, of an ultrafast or ultrashort vortex of topological charge l, or l units of OAM, as the superposition of monochromatic vortex with charge l and varying frequency. The analytical signal complex representation [34] is

$$E = E(\rho,t')e^{il\phi} = \frac{1}{\pi}\int_0^\infty d\omega \hat{E}_\omega(\rho)e^{-i\omega t'}e^{il\phi}. \tag{1}$$

For ultrafast LG vortices of charge l and zero radial order,

$$\hat{E}_\omega(\rho) = \hat{a}_\omega \hat{E}^{\mathrm{LG}}_\omega(\rho) = \hat{a}_\omega D(2\omega\rho^2)^{|l|/2}e^{-\omega\rho^2}, \tag{2}$$

where $\hat{a}_\omega$ specifies the weights or spectrum of monochromatic LG beams, $D = e^{-i(|l|+1)\tan^{-1}(z/z_R)}/\sqrt{1+(z/z_R)^2}$ accounts for Gouy's phase shift and attenuation due to diffraction spreading, z_R is the Rayleigh distance, c is the speed of light in vacuum, $\rho = r/\sqrt{2z_Rc[1+(z/z_R)^2]}$ is a normalized radial coordinate at each propagation distance z, (r,ϕ,z) are cylindrical coordinates, and $t' = t - z/c - \rho^2 z/z_R$ is a local time that is equal to zero at the instant of arrival of the pulse at any position (ρ,z) [30,31]. A constant value of ρ represents the revolution hyperboloid, or caustic surface, $r = \rho\sqrt{2z_Rc[1+(z/z_R)^2]}$ whose revolution axis is the z axis, as illustrated in Fig. 1(a). According to Eqs. (1) and (2), the pulse shape $E(\rho,t')$ only depends on ρ (except for the global complex amplitude factor D) and therefore does not change with propagation distance z along a given revolution hyperboloid.

For *X* waves, or ultrashort *X* vortices of topological charge l, the optical field $E(r,\phi,t,z)$ is given by Eq. (1) with

$$\hat{E}_\omega(\rho) = \hat{a}_\omega \hat{E}^X_\omega(\rho) = \hat{a}_\omega J_l(\omega\rho), \tag{3}$$

where $J_l(x)$ is the Bessel function of the first kind and order l, $\hat{a}_\omega$ is the spectrum of monochromatic Bessel beams, $\rho = (\sin\theta/c)r$, $t' = t - (\cos\theta/c)z$ is the local time for the superluminal propagation at speed $c/\cos\theta$, and θ is the cone angle. The pulse shape changes with the radius ρ, but since *X* waves are diffraction-free, the pulse shape does not change along the cylinders $\rho = \text{const}$ coaxial with the z axis drawn in Fig. 1(b).

For completeness and future generalizations to propagation in linear and nonlinear media, the optical field $E(r,\phi,t,z)$ of ultrashort *X* vortices satisfies the exact wave equation in free space $\Delta E - (1/c^2)\partial_t^2 E = 0$, which written in terms of the local time reads $\Delta E = (2/c)\partial^2_{z,t'}E$. The optical field of ultrashort LG vortices satisfies the paraxial version of the preceding equation, also called the pulsed beam equation

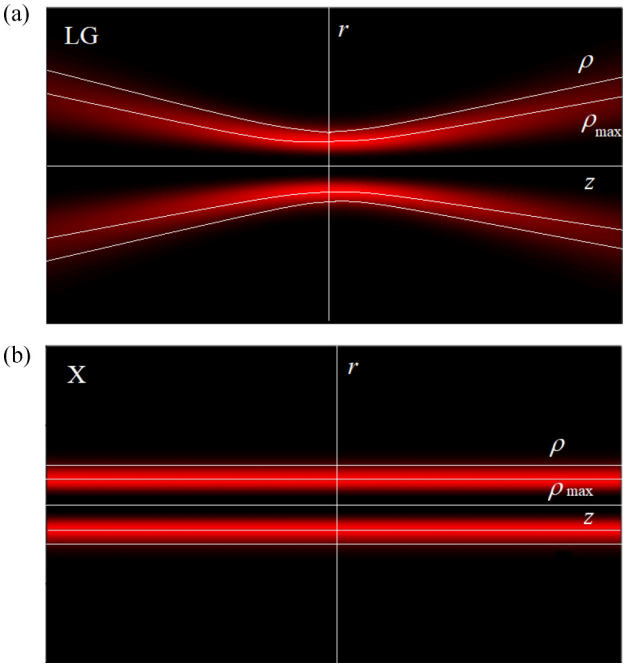

FIG. 1. White curves represent sagittal sections of the revolution hyperboloids $\rho = \text{const}$ of (a) ultrafast LG vortices and (b) cylinders $\rho = \text{const}$ of ultrafast *X* vortices, called here caustic surfaces, along which the pulse shape is invariant. The figures illustrate the geometry of the fluence distribution of both types of vortices.

or paraxial wave equation for ultrashort waveforms [35–37], obtained by neglecting the second derivative with respect to z in the Laplace operator, i.e., $\Delta_\perp E = (2/c)\partial^2_{z,t'}E$, where $\Delta_\perp = \partial_x^2 + \partial_y^2$. The temporal-OAM coupling is a particular spatiotemporal coupling involving the azimuthal and temporal degrees of freedom of the wave. Coupling means here that the azimuthal and temporal structures of the wave are not independent as imposed by the wave equation. Spatiotemporal couplings in the solutions of the wave equation are well known from decades. They are usually small for few-cycle pulses without OAM, e.g., for the fundamental pulsed Gaussian beams [33], although they can be artificially enhanced for practical purposes [38] and appear to be much more pronounced with pulses carrying OAM, as described in [15,30].

Ultrafast LG and *X* vortices with z_R and θ independent of frequency are the only ultrafast vortices that have been described whose temporal shape does not change on propagation (although it changes from one radius to another). In these two types of vortices with propagation-invariant temporal shape, *seemingly discordant* temporal-OAM couplings have been described. The different definitions and dimensions of the normalized radial distance with the same symbol ρ for these two types of ultrashort vortices will help us to visualize more clearly that the temporal-OAM couplings are substantially the same. The limitation to z_R and θ independent of frequency allows us to distinguish the intrinsic and unavoidable effects of OAM on the pulse temporal shape from those arising from propagation in more general models. Mixed propagation-OAM effects on pulse temporal shape in these more general models will be investigated once pure effects of OAM are fully understood.

In the following we will characterize any of the above functions of frequency, say, $\hat{f}_\omega$, by its mean frequency

$$\bar{\omega}_f = \frac{\int_0^\infty d\omega |\hat{f}_\omega|^2 \omega}{\int_0^\infty d\omega |\hat{f}_\omega|^2}, \tag{4}$$

its Gaussian-equivalent half bandwidth

$$\Delta\omega_f = 2\left[\frac{\int_0^\infty d\omega |\hat{f}_\omega|^2 (\omega - \bar{\omega}_f)^2}{\int_0^\infty d\omega |\hat{f}_\omega|^2}\right]^{1/2} \tag{5}$$

(yielding the $1/e^2$ decay of $|\hat{f}_\omega|^2$ for Gaussian-like $\hat{f}_\omega$), and the corresponding pulse shape in the time domain

$$f(t') = \frac{1}{\pi}\int_0^\infty d\omega \hat{f}_\omega e^{-i\omega t'} \tag{6}$$

by its mean time $\bar{t}'_f$ and half duration Δt_f, defined in the same way for $|f(t')|^2$. The term "pulse shape" is often synonymous with pulse (complex) envelope, but our analysis applies also to pulses of duration below the single-cycle regime, as defined in [39], for which the concept of envelope is physically meaningless [39]. Thus, pulse shape will refer to the instantaneous time evolution of the optical signal $f(t')$. For functions that depend also on ρ, we will specify the radius where the above quantities are evaluated, e.g., $\Delta\omega_E(\rho)$ for the bandwidth of $\hat{E}_\omega(\rho)$ at ρ or $\Delta t_E(\rho)$ for the duration of $E(\rho, t')$ at ρ.

III. TEMPORAL-OAM COUPLINGS AT THE BRIGHT CAUSTIC SURFACE

In experiments involving nonlinear interactions, the region in the transversal plane where the pulse energy is high is the most relevant. Following Refs. [30,31] we consider the energy density

$$\mathcal{E}(\rho) = \int_{-\infty}^\infty dt' (\mathrm{Re}E)^2 = \frac{1}{2}\int_{-\infty}^\infty dt' |E|^2 = \frac{1}{\pi}\int_0^\infty d\omega |\hat{E}_\omega(\rho)|^2, \tag{7}$$

whose typical spatial distribution is shown in Fig. 1, and analyze the pulse properties at the hyperbolic or cylindrical caustic surface $\rho_{\max}$, where the energy density is maximum, or bright caustic surface. As seen in the examples of Figs. 2(a) and 3(a), $\rho_{\max}$ increases monotonically with $|l|$.

A. Ultrafast LG vortices

A fundamental restriction on the pulse characteristics at the bright caustic surface of all ultrafast LG vortices has been described recently [31]. With given topological charge l, the relative spectral bandwidth of the pulse at the bright caustic surface necessarily satisfies the inequality $\Delta\omega_E(\rho_{\max})/\bar{\omega}_E(\rho_{\max}) \leqslant 2/\sqrt{|l|}$. More recently, the mean frequency of the oscillations at this caustic, $\bar{\omega}_E(\rho_{\max})$, has been shown to coincide with the mean frequency $\bar{\omega}_a$ of the spectrum of LG beams $\hat{a}_\omega$ in the particular situation that $\hat{a}_\omega$ is chosen to be a power-exponential spectrum [30], but, as argued below, the approximate equality $\bar{\omega}_E(\rho_{\max}) \simeq \bar{\omega}_a$ holds with generality. Thus, in practice, all ultrafast LG vortices

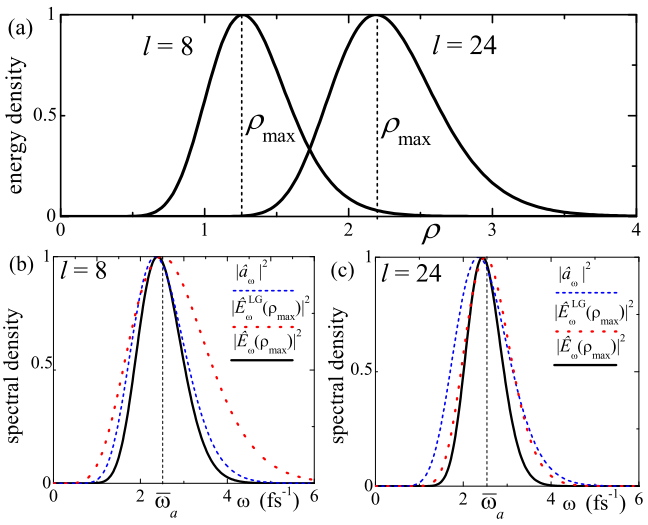

FIG. 2. Ultrashort LG vortices at their bright caustic surface. In these two examples $\hat{a}_\omega = \omega^{7.5}e^{-3.2\omega}$, yielding about a single-cycle pulse in the time domain of mean frequency $\bar{\omega}_a = 2.5$ fs^{-1} in the near infrared. (a) Energy density radial profiles for $l = 8$ and 24. The vertical lines are located at $|l^2|/2\omega_a$, which accurately locate $\rho_{\max}$. (b) and (c) Factors $|\hat{a}_\omega|^2$ (dashed blue curve) and $|\hat{E}^{\mathrm{LG}}_\omega(\rho_{\max})|^2$ (dotted red curve) of the spectral density $|\hat{E}_\omega(\rho_{\max})|^2$ (solid black curve) at the bright caustic. Since absolute values are irrelevant, all functions are normalized to their peak values.

satisfy

$$\frac{\Delta\omega_E(\rho_{\max})}{\bar{\omega}_a} \lesssim \frac{2}{\sqrt{|l|}}. \tag{8}$$

Since $\Delta t_f \Delta\omega_f \gtrsim 2$ for any pair $\hat{f}_\omega$ and $f(t')$, the approximate equality being reached only for Gaussian-like f_ω, it follows that the duration of the pulse at the bright caustic is restricted by $\Delta t_E(\rho_{\max}) \gtrsim \sqrt{|l|}/\bar{\omega}_E(\rho_{\max})$. On account that $\bar{\omega}_E(\rho_{\max}) \simeq \bar{\omega}_a$, the lower bound to the pulse duration at the bright caustic is in practice

$$\Delta t_E(\rho_{\max}) \gtrsim \frac{\sqrt{|l|}}{\bar{\omega}_a}. \tag{9}$$

For a particular application, one may wish to fix a pulse shape of certain characteristics at the bright caustic. The above restrictions then impose that the topological charge of an ultrafast vortex with such a pulse shape has the upper bound $|l| \lesssim [\bar{\omega}_E^2(\rho_{\max})\Delta t_E^2(\rho_{\max})]$, where the square brackets mean the integer part. A consequence of the dependence on l of the lower bound to the pulse duration in the inequality (9) is that the pulse at the bright caustic of the ultrafast LG vortex synthesized with the same spectrum $\hat{a}_\omega$ necessarily broadens with increasing magnitude of the topological charge. This temporal-OAM coupling effect was recently verified in [30] with a particular choice of $\hat{a}_\omega$. These bounds settle unavoidable limits, for example, to the velocity of information transmission or to the number of channels in communication systems based on ultrashort pulses carrying OAM.

An intuitive explanation of these temporal-OAM coupling effects for ultrashort LG vortices with general $\hat{a}_\omega$ (and that apply also to the ultrashort X vortices considered below) is

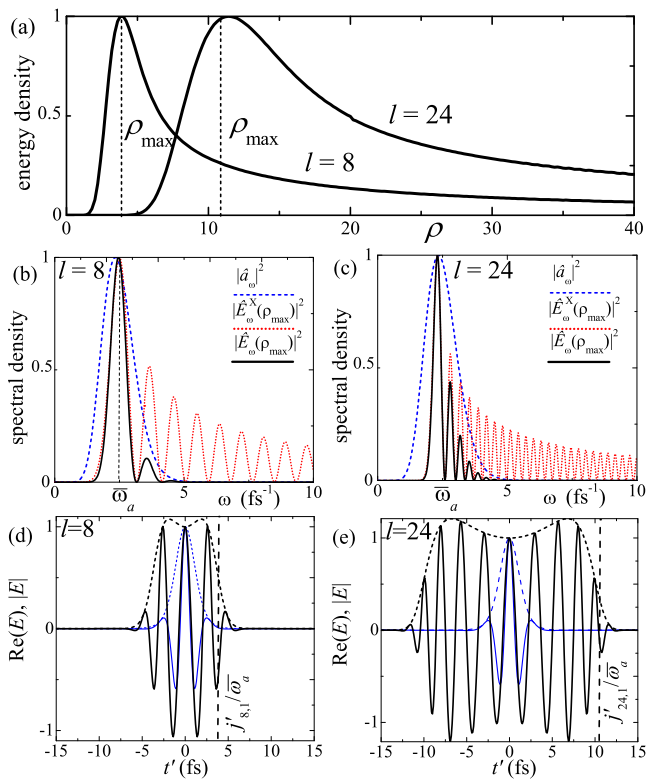

FIG. 3. Ultrafast X vortices at their bright caustic surface. In these two examples $\hat{a}_\omega = \omega^{7.5}e^{-3.2\omega}$, as for the ultrafast LG vortices of Fig. 2 (about a single-cycle pulse of mean frequency $\bar{\omega}_a = 2.5$ fs^{-1}). (a) Energy density radial profiles for $l = 8$ and 24. The vertical lines are located at $j'_{l,1}/\bar{\omega}_a$ and approximate ρ_{max}. (b) and (c) Factors $|\hat{a}_\omega|^2$ (dashed blue curve) and $|\hat{E}^X_\omega(\rho_{max})|^2$ (dotted red curve) of the spectral density $|\hat{E}_\omega(\rho_{max})|^2$ (black curve) at the bright caustic. Since absolute values are irrelevant, all functions are normalized to their peak values. (d) and (e) Real field and envelope of the pulse with the spectrum $\hat{a}_\omega$ (thin solid and dashed curves) and of the X wave with the same spectrum and $l = 8$ and with $l = 24$ at their bright caustic (thick solid and dashed curves). All functions are normalized to the value at $t' = 0$.

as follows. The spectral density of the ultrafast LG vortex in (2) is the product of $|\hat{a}_\omega|^2$, centered about $\bar{\omega}_a$, and $|\hat{E}^{\rm LG}_\omega(\rho)|^2$, characterized by a single maximum at $\omega_M = |l|/2\rho^2$. At arbitrary ρ these two functions of frequency do not overlap. The energy density in Eq. (7) is maximum at ρ_{max} because these two functions overlap optimally at this radius, as in the examples of Figs. 2(b) and 2(c), which implies that the mean frequency of the ultrafast LG vortex at the bright caustic $\bar{\omega}_E(\rho_{max})$ is approximately equal to ω_M and to $\bar{\omega}_a$, i.e., no significant blueshift or redshift of the mean frequency at the bright caustic is expected, as described in [31] for a specific $\hat{a}_\omega$. The relation $\bar{\omega}_a \simeq \omega_M = |l|/2\rho^2_{max}$ provides the approximate expression $\rho^2_{max} \simeq |l|/2\bar{\omega}_a$ for the location of the bright, as verified in the examples of Fig. 2(a). At this radius $|\hat{E}^{\rm LG}_\omega(\rho_{max})|^2 = |l|^{|l|}(\omega/\bar{\omega}_a)^{|l|}e^{-|l|\omega/\bar{\omega}_a}$ is an approximate Gaussian function, especially for large $|l|$, of Gaussian width $\Delta\omega_{\rm LG}(\rho_{max}) \simeq 2\bar{\omega}_a/\sqrt{|l|}$. Thus, as the product of $|\hat{a}_\omega|^2$ and $|\hat{E}^{\rm LG}_\omega(\rho_{max})|^2$, the spectral density $|\hat{E}_\omega(\rho_{max})|^2$ cannot be wider than $|\hat{E}^{\rm LG}_\omega(\rho_{max})|^2$, i.e., $\Delta\omega_E(\rho_{max}) \leqslant \Delta\omega_{\rm LG}(\rho_{max})$, or $\Delta\omega_E(\rho_{max})/\bar{\omega}_a \lesssim 2/\sqrt{|l|}$ and $\Delta t_E(\rho_{max}) \gtrsim \sqrt{|l|}/\bar{\omega}_a$, as in the inequalities (8) and (9). Although approximate equalities are used in this derivation, the result is the same as the one rigorously derived in [30]. Also, with given $\hat{a}_\omega$ the condition $\Delta t_E(\rho_{max}) \gtrsim \sqrt{|l|}/\bar{\omega}_a$ implies that the pulse duration at the bright caustic necessarily increases from the lowest value Δt_a (for $l = 0$) as $|l|$ increases, as described in [31] but for general $\hat{a}_\omega$.

B. Ultrafast X vortices

Similar reasonings applied to ultrafast X vortices, or the X wave with OAM, allowing us to conclude that temporal-OAM couplings at their cylindrical caustic surface of maximum energy density are qualitatively similar. In particular, there is a lower bound to their duration.

Figure 3(a) shows two radial profiles of the energy density featuring single maxima at certain radii ρ_{max} that increase with $|l|$. The spectral density of the ultrashort X vortex is also the product of $|\hat{a}_\omega|^2$ and $|\hat{E}^X_\omega(\rho)|^2 = J^2_l(\omega\rho)$, the latter characterized by an absolute maximum at $\omega_M = j'_{l,1}/\rho$, where $j'_{l,1} \simeq |l| + 0.808\,69|l|^{1/3}$ is the location of the first maximum of $J_l(x)$ [40]. As illustrated in Figs. 3(b) and 3(c), optimum overlapping of these two functions at the radius ρ_{max} of maximum energy density implies again that $\bar{\omega}_E(\rho_{max}) \simeq \bar{\omega}_X(\rho_{max}) \simeq \bar{\omega}_a$. We then do not expect a significant redshift or blueshift of the mean frequency at the bright caustic with respect to the value $\bar{\omega}_a$ determined by the spectrum of Bessel beams, such as for ultrashort LG vortices [31] and at variance with ultrashort X vortices in the neighborhood of their vortex [15]. The relation $\rho_{max} \simeq j'_{l,1}/\bar{\omega}_a$ provides an approximation to the location of the bright caustic, as is verified in Fig. 3(a). As the product of $\hat{a}_\omega$ and $|\hat{E}^X_\omega(\rho_{max})|^2 = J^2_l(\omega j'_{l,1}/\bar{\omega}_a)$, the full spectral density $|\hat{E}_\omega(\rho_{max})|^2$ at the bright caustic cannot be wider than $J^2_l(\omega j'_{l,1}/\bar{\omega}_a)$, approaching it only with wider and wider $|\hat{a}_\omega|^2$, in which case the narrowest pulse at the bright caustic is $E(\rho_{max}, t') = (1/\pi)\int_0^\infty d\omega J_l(\omega\rho_{max})e^{-i\omega t'}$ with $\rho_{max} \simeq j'_{l,1}/\bar{\omega}_a$, i.e.,

$$E(\rho_{max}, t') = \lim_{\epsilon\to 0} \frac{\left[\sqrt{(\epsilon + it')^2 + \rho^2_{max}} - (\epsilon + it')\right]^{|l|}}{\pi\,\rho^{|l|}_{max}\sqrt{(\epsilon + it')^2 + \rho^2_{max}}} \quad (10)$$

for $l > 0$, and multiplied by $(-1)^{|l|}$ for $l < 0$, with $\rho_{max} \simeq j'_{l,1}/\bar{\omega}_a$. As can be clearly seen in Fig. 4, the half duration of the pulses in Eq. (10) is $\Delta t = \rho_{max}$; hence the minimum pulse duration at the bright caustic of an ultrashort X vortex with l units of OAM is $\rho_{max} \simeq j'_{l,1}/\bar{\omega}_a$. In conclusion, for any other ultrashort X vortex

$$\Delta t_E(\rho_{max}) \gtrsim \frac{j'_{l,1}}{\bar{\omega}_a} \simeq \frac{|l| + 0.808\,69|l|^{1/3}}{\bar{\omega}_a} \simeq \frac{|l|}{\bar{\omega}_a}, \quad (11)$$

the last approximate equality being valid for large $|l|$. Also, the l dependence of this lower bound implies that with given $\hat{a}_\omega$ the pulse shape at the bright caustic must necessarily increase as $|l|$ grows; indeed, it must do so almost linearly above a certain value of $|l|$. This description of the temporal-OAM coupling effects at the bright caustic of ultrashort X vortices complements the temporal-OAM coupling effects close to the vortex described in [15] and its validity is tested in the examples of Figs. 3(d) and 3(e). With the same spectrum $\hat{a}_\omega$ of

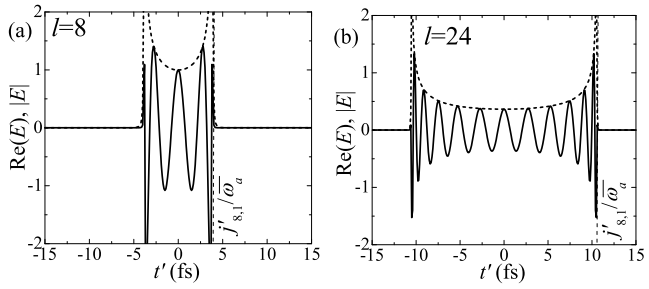

FIG. 4. Real field (solid curve) and modulus (dashed curve) of minimal pulse shapes at the bright caustic of ultrafast X vortices as given by Eq. (10) with $\rho_{\max} = j'_{l,1}/\bar{\omega}_a$ and $\bar{\omega}_a = 2.5$ fs^{-1}. Their half duration is just $\rho_{\max}$.

about a single-cycle pulse (blue curves), the mean frequency at the bright caustic does not significantly depart from $\bar{\omega}_a$ as $|l|$ grows (black curves), but the number of oscillations increases with $|l|$ so that the pulse duration is always above $j'_{l,1}/\bar{\omega}_a$ (vertical dashed lines). Broadening is very small for durations Δt_a of $a(t')$ well above the lower bound, i.e., for $\Delta t_a \gg j'_{l,1}/\bar{\omega}_a$, but is very pronounced for $\Delta t_a \lesssim j'_{l,1}/\bar{\omega}_a$, as in Figs. 3(d) and 3(e), in which case the pulse shape is an apodized nonsingular version of the minimal pulse shape in Fig. 4.

As a partial conclusion, the temporal-OAM coupling effects at the more energetic caustic in the only two known cases of ultrafast vortices with propagation-invariant pulse shape are qualitatively similar. In particular, the mean or carrier frequency of $\hat{a}_\omega$ (which can be identified with the frequency of the laser source) is also the observable carrier frequency at the bright caustic of the produced ultrafast LG or X vortex. For ultrashort X vortices there also exists a lower bound to their duration at their bright caustic. Temporal broadening with increasing magnitude of the topological charge is more pronounced for X vortices than for LG vortices because of the respective square root [Eq. (9)] and almost linear dependence [Eq. (11)] of the lower bound to the temporal duration.

IV. TEMPORAL-OAM COUPLINGS IN THE NEIGHBORHOOD OF THE VORTEX

The low-intensity region close to the vortex is of interest in quantum optics. Spectral anomalies in the vicinity of vortices of continuous, coherent, and incoherent light were studied in [41]. Temporal-OAM coupling effects in the vicinity of the vortex of X waves were analyzed in detail in [15,16]. It turns out from our analysis that these temporal-OAM coupling effects are qualitatively the same for ultrashort LG vortices in the proper spatial regions.

In the vicinity of the vortex, monochromatic LG beams behave asymptotically as $\hat{E}^{\rm LG}_\omega(\rho) \simeq (\omega\rho^2)^{|l|/2}$ and monochromatic Bessel beams as $\hat{E}^{X}_\omega(\rho) \simeq (\omega\rho)^{|l|}$ (aside from an irrelevant constant). The complete spectra are then $\hat{E}_\omega(\rho) \simeq \hat{a}_\omega(\omega\rho^2)^{|l|/2}$ for ultrashort X vortices and $\hat{E}_\omega(\rho) \simeq \hat{a}_\omega(\omega\rho)^{|l|}$ for ultrashort X vortices.

For the analysis below, we define

$$\bar{\omega}(m) = \frac{\int_0^\infty d\omega |\hat{a}_\omega|^2 \omega^{m+1}}{\int_0^\infty d\omega |\hat{a}_\omega|^2 \omega^m} \tag{12}$$

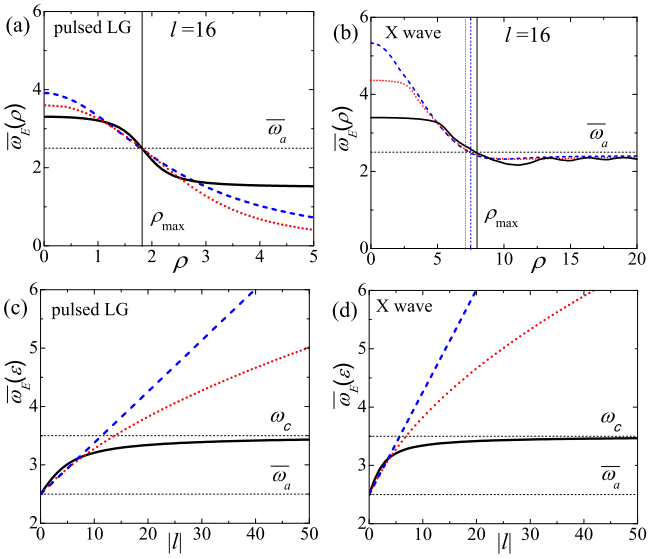

FIG. 5. Behavior close to the vortex. Mean frequencies of ultrashort LG and X vortices are shown for three different spectra $\hat{a}_\omega$: power-exponential $\hat{a}_\omega \propto \omega^{\alpha-1/2}\exp(-\alpha\omega/\bar{\omega}_a)$ with $\alpha = 14.24$ (dashed blue curves), Gaussian $\hat{a}_\omega \propto \exp[-(\omega-\bar{\omega}_a)^2/\Delta\omega_a^2]$ with $\Delta\omega_a \simeq 1$ fs^{-1} (red dotted curves), and square $\hat{a}_\omega \propto 1$ if $|\omega - \bar{\omega}_a| < \delta\omega$ and 0 otherwise, with $\delta\omega \simeq 1$ fs^{-1} (black solid curves), all with the same mean frequency $\bar{\omega}_a = 2.5$ fs^{-1}. The three spectra correspond to single-cycle pulses $a(t')$ [one oscillation in the full width at half-maximum of the cycle-averaged intensity $|a(t')|^2$] of different shapes. The mean frequency is shown as a function of radial distance for ultrashort (a) LG and (b) X vortices with $l = 16$. The radius $\rho_{\max}$ is almost independent of these three spectral shapes for LG vortices and appreciably varies with spectral shape for X vortices (vertical lines). The mean frequency is shown also in the vicinity of the vortex $\rho = \epsilon$ for ultrafast (c) LG and (d) X vortices with the above spectral shapes $\hat{a}_\omega$ as functions of the magnitude of the topological charge $|l|$.

for any natural number m, with the dimensions of a frequency. In particular, $\bar{\omega}(0) = \bar{\omega}_a$. It can be readily seen that the combination $\bar{\omega}(m)[\bar{\omega}(m+1) - \bar{\omega}(m)]$ is the variance of the distribution $|\hat{a}_\omega|^2\omega^m$ and as such is positive (except if $\hat{a}_\omega$ contains a single frequency). It then follows that $\bar{\omega}(m)$ is a strictly growing function of m if $\hat{a}_\omega$ is not a monochromatic spectrum. For all bell-shaped spectral shapes $\hat{a}_\omega$ of interest, $\bar{\omega}(m)$ is a concave function of m and therefore $\bar{\omega}(m+1)/\bar{\omega}(m)$ approaches unity from above as m increases.

In [15] a linear increase of the mean frequency about the vortex of ultrafast X vortices with a power-exponential spectrum $\hat{a}_\omega$ was predicted. Growth of the mean frequency is a general feature, also for ultrafast LG vortices. Figures 5(a) and 5(b) illustrate the behavior of the mean frequency as a function of the radial distance ρ from the vortex for ultrafast LG and X vortices with three different choices of $\hat{a}_\omega$, all three corresponding to single-cycle pulses of different shapes (power-exponential, Gaussian, and square spectra in a certain bandwidth; see the caption for details). The mean frequency is always seen to grow from $\bar{\omega}_a$ at the bright caustic up to a locally constant value in the vicinity of the vortex. Indeed, with the spectral densities $|\hat{E}_\omega(\rho)|^2 \simeq |\hat{a}_\omega|^2(\omega\rho^2)^{|l|}$ and $|\hat{E}_\omega(\rho)|^2 \simeq |\hat{a}_\omega|^2(\omega\rho)^{2|l|}$ of ultrafast LG and X vortices

close to the vortex, the mean frequency in this region is found to be

$$\bar{\omega}_E(\epsilon) = \bar{\omega}(|l|), \quad \bar{\omega}_E(\epsilon) = \bar{\omega}(2|l|) \tag{13}$$

(ϵ stands for $\rho \to 0$) in the respective cases of ultrashort LG and X vortices. Thus, for $|l| > 0$, $\bar{\omega}_E(\epsilon) > \bar{\omega}(0) = \bar{\omega}_a$ for general $\hat{a}_\omega$, i.e., there is always a blueshift towards the vortex center and this blueshift is more pronounced for X vortices than for LG vortices. Small blueshifts of the carrier oscillations have been previously described, for example, for pulsed Gaussian beams about the beam axis at the far field [42–44]. Here the on-axis blueshift is permanent along the propagation direction and is monotonically enhanced as the magnitude of the topological charge $|l|$ increases, as illustrated in Figs. 5(c) and 5(d) for the same three particular spectra of single-cycle pulses. For spectra without a cutoff frequency, such as the power-exponential and Gaussian spectra, the mean frequency about the vortex grows without bound with the magnitude of the topological charge and for spectra with a cutoff frequency ω_c grows up to it. These huge blueshifts should be observable in experiments, e.g., with the spectral bandwidth of a single-cycle pulse in the near infrared and topological charge $|l| = 20$; the mean frequency in the bright caustic is indeed in the near infrared, but is in the visible region or in the ultraviolet close to the vortex of ultrashort LG and X vortices.

Also in [15], a slow shortening of the pulse with increasing $|l|$ close to the vortex of ultrashort X vortices with power-exponential spectra is reported, which together with the more pronounced decrease of the mean period $2\pi/\bar{\omega}_E(\epsilon)$ results in an increase of the number of oscillations with as $|l|$ grows. This effect is seen here to be almost identical for ultrashort LG vortices with power-exponential spectra. However, it also follows also from our analysis that pulse shortening or lengthening is not a general temporal-OAM coupling effect, but is dictated by the particular spectrum $\hat{a}_\omega$, and that the only two general temporal-OAM coupling effects close to the vortex are a blueshift and an increase of the number of oscillations with $|l|$. In a sense, ultrafast LG and X vortices always approach a monochromatic behavior in the vicinity of the vortex as their topological charge increases.

Indeed, the definition of bandwidth in Eq. (5) for the spectra $\hat{E}_\omega(\rho)$ of ultrafast LG and X vortices close to the center leads to the expressions of the bandwidth

$$\Delta\omega_E(\epsilon) = 2\sqrt{\bar{\omega}(|l|)[\bar{\omega}(|l|+1) - \bar{\omega}(|l|)]}, \tag{14}$$

$$\Delta\omega_E(\epsilon) = 2\sqrt{\bar{\omega}(2|l|)[\bar{\omega}(2|l|+1) - \bar{\omega}(2|l|)]} \tag{15}$$

for ultrafast LG and X vortices, respectively. As in the examples in Fig. 6(a) with the same three spectral shapes $\hat{a}_\omega$ of single-cycle pulses as in Fig. 5, the bandwidth close to the vortex may increase with $|l|$, decrease, or reach a constant value, the corresponding pulse durations then behaving in reverse, as illustrated in Figs. 6(c)–6(e) for the three types of spectral shapes. However, the relative bandwidths

$$\frac{\Delta\omega_E(\epsilon)}{\bar{\omega}_E(\epsilon)} = 2\sqrt{\frac{\bar{\omega}(|l|+1)}{\bar{\omega}(|l|)} - 1}, \tag{16}$$

$$\frac{\Delta\omega_E(\epsilon)}{\bar{\omega}_E(\epsilon)} = 2\sqrt{\frac{\bar{\omega}(2|l|+1)}{\bar{\omega}(2|l|)} - 1} \tag{17}$$

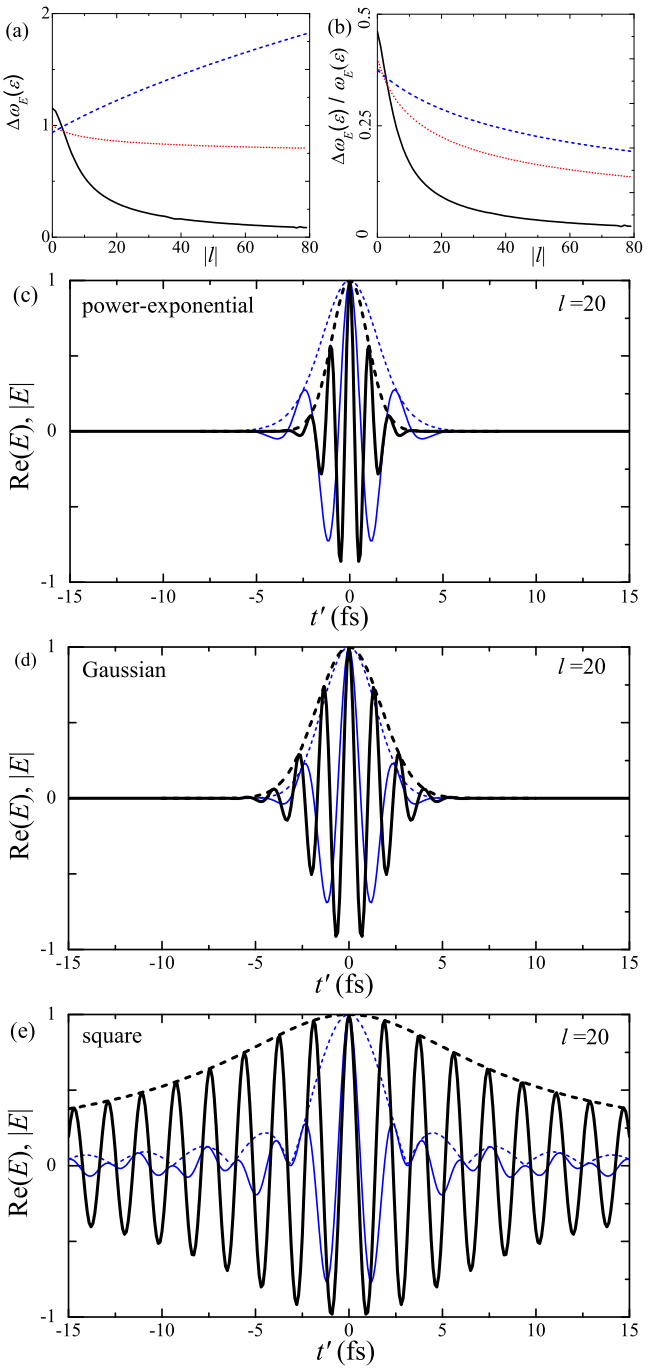

FIG. 6. Behavior close to the vortex. Bandwidths and relative bandwidths of ultrashort LG vortices are shown with the same power-exponential (dashed blue curve), Gaussian (dotted red curve), and square (solid black curve) spectra $\hat{a}_\omega$ as in Fig. 5, all corresponding to single-cycle pulses $a(t')$ of the same mean frequency $\bar{\omega}_a = 2.5\ \mathrm{fs}^{-1}$. (a) Bandwidth and (b) relative bandwidth as functions of the magnitude of the topological charge. (c)–(e) Pulse shapes and envelopes for $l = 20$ close to the vortex in the above three cases (thick black curves), compared to the single-cycle pulses $a(t')$ (thin blue curves). Depending on the specific $a(t')$, the pulse may broaden or shrink with $|l|$, but the number of oscillations always grows with $|l|$.

for ultrafast LG and X vortices, respectively, always go to zero with growing $|l|$, as in Fig. 6(b), since $\bar{\omega}(m+1)/\bar{\omega}(m)$

approaches unity with increasing m. Hence, the number N of mean or carrier periods $2\pi/\bar{\omega}_E(\epsilon)$ in the full pulse duration $2\Delta t_E(\epsilon)$, with $\Delta t_E(\epsilon) \geqslant 2/\Delta\omega_E(\epsilon)$ or $N = \Delta t_E(\epsilon)\bar{\omega}_E(\epsilon)/\pi$, always satisfies $N \geqslant (2/\pi)\bar{\omega}_E(\epsilon)/\Delta\omega_E(\epsilon)$, with the right-hand side of the inequality growing without bound with increasing $|l|$, regardless of the choice of $\hat{a}_\omega$. This is why the pulse shapes close to the vortex in Figs. 6(c)–6(e) always contain more oscillations than $a(t')$, despite the pulse being longer or shorter.

V. CONCLUSION

In this paper we have reported a unified treatment of ultrashort vortices with propagation-invariant temporal shape for studying the universal and diverse forms of their coupling between the temporal and orbital angular momentum degrees of freedom, a kind of spatiotemporal coupling peculiar to ultrashort vortices. This study completes previous studies and clarifies their seemingly contradictory results.

We have shown that orbital angular momentum introduces a strong correlation between the amount of spatial twisting, the local frequency, and the pulse duration. The coupling manifests itself in two ways in different regions of the three-dimensional energy distribution. In the high-intensity caustic surface surrounding the vortex, the l-dependent lower bound to the pulse duration previously reported for ultrashort LG vortices holds similarly for ultrashort X vortices. As a consequence, the pulse duration of both ultrashort LG and X vortices must increase with the angular momentum. This fact may have an impact on multilevel-OAM pulsed transmission systems. In the low-intensity region, in the proximity of the vortex phase singularity, we found that a blueshift with an increase of the number of oscillations with respect to those at the bright caustic surface occurs not only for ultrashort X vortices, as previously reported, but also for ultrashort LG vortices. Pulse shortening or lengthening in the vicinity of the vortex is not a general feature of the temporal-OAM coupling, but depends on the particular model. Higher frequencies are then located in low-energy-density regions close to the vortex. The local blueshift increases with the topological charge and is larger for ultrafast X vortices than for LG vortices.

It is an open question if this remarkable space-time correlation in the dark regions has fundamental implications in quantum optics at the single-photon level or for entangled beams. We think that the blueshift can be measured with synthesized propagation-invariant pulses, ranging from terahertz to visible. We also believe that the frequency shift may be evident in high-field phenomena, as in high-harmonic generation, where the amount of angular momentum grows with the harmonic order and where, so far, spatiotemporal coupling effects and the internal structure of the generated beams have been overlooked.

ACKNOWLEDGMENTS

This research was funded by Spanish Ministerio de Economía y Competitividad, Grants No. PGC2018-093854-B-I00 and No. FIS2017-87360-P.

[1] J. Lu and J. F. Greenleaf, Nondiffracting X waves-exact solutions to free-space scalar wave equation and their finite aperture realizations, IEEE Trans. Ultrason. Ferr. Freq. Control **39**, 19 (1992).

[2] P. Saari and K. Reivelt, Evidence of X-Shaped Propagation-Invariant Localized Light Waves, Phys. Rev. Lett. **79**, 4135 (1997).

[3] *Localized Waves*, edited by H. E. Hernandez-Figueroa, M. Zamboni-Rached, and E. Recami (Wiley, New York, 2008).

[4] I. Bialynicki-Birula, Photon wave function, Prog. Opt. **36**, 245 (1996).

[5] P. Saari, How small a packet of photons can be made?, Laser Phys. **16**, 556 (2006).

[6] P. Saari, O. Rebane, and I. Besieris, Energy-flow velocities of nondiffracting localized waves, Phys. Rev. A **100**, 013849 (2019).

[7] J. Lu, and S. He, Optical X wave communications, Opt. Commun. **161**, 187 (1999).

[8] H. E. Kondakci and A. F. Abouraddy, Optical space-time wave packets having arbitrary group velocities in free space, Nat. Commun. **10**, 929 (2019).

[9] C. Conti and S. Trillo, Nonspreading Waves Packets in Three Dimensions Formed by an Ultracold Bose Gas in an Optical Lattice, Phys. Rev. Lett. **92**, 120404 (2004).

[10] C. Conti, S. Trillo, P. Di Trapani, G. Valiulis, A. Piskarskas, O. Jedrkiewicz, and J. Trull, Nonlinear Electromagnetic X Waves, Phys. Rev. Lett. **90**, 170406 (2003).

[11] M. Porras, S. Trillo, C. Conti, and P. Di Trapani, Paraxial envelope X-waves, Opt. Lett. **28**, 1090 (2003).

[12] A. Gianfrate, L. Dominici, O. Voronych, M. Matuszewski, M. Stobińska, D. Ballarini, M. De Giorgi, G. Gigli, and D. Sanvitto, Superluminal X-waves in a polariton quantum fluid, Light Sci. Appl. **7**, 17119 (2018).

[13] D. Colas, F. P. Laussy, and M. J. Davis, Formation of nonlinear X-waves in condensed matter systems, Phys. Rev. B **99**, 214301 (2019).

[14] J. N. Steer, A. G. L. Borthwick, M. Onorato, A. Chabchoub, and T. S. van den Bremer, Hydrodynamic X waves, Phys. Rev. Lett. **123**, 184501 (2019).

[15] M. Ornigotti, C. Conti, and A. Szameit, Effect of Orbital Angular Momentum on Nondiffracting Ultrashort Optical Pulses, Phys. Rev. Lett. **115**, 100401 (2015).

[16] M. Ornigotti, C. Conti, and A. Szameit, Universal form of the carrier frequency of scalar and vector paraxial X waves with orbital angular momentum and arbitrary frequency spectrum, Phys. Rev. A **92**, 043801 (2015).

[17] A. Ciattoni and C. Conti, Quantum electromagnetic X waves, J. Opt. Soc. Am. B **24**, 2195 (2007).

[18] M. Ornigotti, L. D. M. Villari, A. Szameit, and C. Conti, Squeezing of X waves with orbital angular momentum, Phys. Rev. A **95**, 011802(R) (2017).

[19] L. Rego *et al.*, Generation of extreme-ultraviolet beams with time-varying orbital angular momentum, Science **364**, 1253 (2019).

[20] G. Gariepy, J. Leach, K. T. Kim, T. J. Hammond, E. Frumker, R. W. Boyd, and P. B. Corkum, Creating High-Harmonic Beams with Controlled Orbital Angular Momentum, Phys. Rev. Lett. **113**, 153901 (2014).

[21] C. Hernández-García, A. Picón, J. San Román, and L. Plaja, Attosecond Extreme Ultraviolet Vortices from High-Order Harmonic Generation, Phys. Rev. Lett. **111**, 083602 (2013).

[22] R. Gńeaux, A. Camper, T. Auguste, O. Gobert, J. Caillat, R. Taïeb, and T. Ruchon, Synthesis and characterization of attosecond light vortices in the extreme ultraviolet, Nat. Commun. **7**, 12583 (2016).

[23] L. Rego, J. San Román, A. Picón, L. Plaja, and C. Hernández-García, Nonperturbative Twist in the Generation of Extreme-Ultraviolet Vortex Beams, Phys. Rev. Lett. **117**, 163202 (2016).

[24] K. Bezuhanov, A. Dreischuh, G. G. Paulus, M. G. Schätzel, and H. Walther, Vortices in femtosecond laser fields, Opt. Lett. **29**, 1942 (2004).

[25] I. Zeylikovich, H. I. Sztul, V. Kartazaev, T. Le, and R. R. Alfano, Ultrashort Laguerre-Gaussian pulses with angular and group velocity dispersion compensation, Opt. Lett. **32**, 2025 (2007).

[26] Y. Tokizane, K. Oka, and R. Morita, Supercontinuum optical vortex pulse generation without spatial or topological-charge dispersion, Opt. Express **17**, 14517 (2009).

[27] V. G. Shvedov, C. Hnatovsky, W. Krolikowski, and A. V. Rode, Efficient beam converter for the generation of high-power femtosecond vortices, Opt. Lett. **35**, 2660 (2010).

[28] A. Richter, M. Bock, J. Jahns, and R. Grunwald, Orbital angular momentum experiments with broadband few cycle pulses, in *Complex Light and Optical Forces IV*, edited by E. J. Galvez, D. L. Andrews, and J. Glückstad, *SPIE Proc. Vol.* 7613 (SPIE, Bellingham, 2010), p. 761308.

[29] K. Yamane, Y. Toda, and R. Morita, Ultrashort optical-vortex pulse generation in few-cycle regime, Opt. Express **20**, 18986 (2012).

[30] M. A. Porras, Upper Bound to the Orbital Angular Momentum Carried by an Ultrashort Pulse, Phys. Rev. Lett. **122**, 123904 (2019).

[31] M. A. Porras, Effects of orbital angular momentum on few-cycle and sub-cycle pulse shapes: Coupling between the temporal and angular momentum degrees of freedom, Opt. Lett. **44**, 2538 (2019).

[32] M. A. Porras, Attosecond helical pulses, Phys. Rev. A **100**, 033826 (2019).

[33] M. A. Porras, Ultrashort pulsed Gaussian beams, Phys. Rev. E **58**, 1086 (1998).

[34] M. Born and E. Wolf, *Principles of Optics* (Pergamon, Oxford, 1975).

[35] E. Heyman, Pulsed beam propagation in inhomogeneous medium, IEEE Trans. Antennas Propag. **42**, 311 (1994).

[36] M. A. Porras, Nonsinusoidal few-cycle pulsed light beams in free space, J. Opt. Soc. Am. B **16**, 1468 (1999).

[37] I. M. Besieris and A. M. Shaarawi, Paraxial localized waves in free space, Opt. Express **12**, 3848 (2004).

[38] S. Akturk, X. Gu, P. Bowlan, and R. Trebino, Spatio-temporal couplings in ultrashort laser pulses, J. Opt. **12**, 093001 (2010).

[39] T. Brabec and F. Krausz, Nonlinear Optical Pulse Propagation in the Single-Cycle Regime, Phys. Rev. Lett. **78**, 3282 (1997).

[40] *NIST Handbook of Mathematical Functions*, F. W. Olver, D. Lozier, R. F. Boisvert, and C. W. Clark (Cambridge University Press, Cambridge, 2010).

[41] V. Klimov, D. Bloch, M. Ducloy, and J. R. R. Leite, Detecting photons in the dark region of Laguerre-Gauss beams, Opt. Express **17**, 9718 (2009).

[42] C. J. R. Sheppard and X. Gan, Free-space propagation of femtosecond light pulses, Opt. Commun. **133**, 1 (1997).

[43] A. E. Kaplan, Diffraction-induced transformation of near-cycle and subcycle pulses, J. Opt. Soc. Am. B **15**, 951 (1998).

[44] M. A. Porras, Diffraction effects in few-cycle optical pulses, Phys. Rev. E **65**, 026606 (2002).